Stress-Induced Relapse to Nicotine Seeking: Mechanistic Effect of Guanfacine in Male Mice

Ashna Aggarwal

Advised by Dr. Marina Picciotto, PhD

Yale University

April 24, 2020

Contents

Abstract

Relapse to smoking occurs at high rates, however novel therapies may increase rates of successful abstinence by targeting specific triggers of relapse, such as stress. Human studies have shown that the α_2-adrenergic receptor agonist guanfacine can decrease stress-induced relapse to smoking, and a recent preclinical study from my lab has shown that guanfacine attenuates stress-induced reinstatement of nicotine conditioned place preference (CPP), an animal model of drug-seeking behavior, in male and female mice. Along with these behavioral findings, immunohistochemistry experiments showed lowered activity in the anterior insular cortex (AI) region of male mice, as indicated by Arc expression. Importantly, the overall count of Arc-immunoreactive (Arc-ir) cells doesn't elucidate potential cell-type specific mechanisms by which guanfacine may be attenuating reinstatement of nicotine CPP in male mice. To investigate these mechanisms, I examined the activity of two neuron types, marked by the presence of calcium/calmodulin-dependent protein kinase IIα (CaMKIIα-ir) and parvalbumin (PV-ir), in the AI. My investigation focused on male mice, and consisted of behavioral conditioning, immunohistochemistry, imaging, and data analysis in a 2x2 design (nicotine-treated vs. saline-treated, and injection of guanfacine vs. saline before stress). Two main findings are presented: first, a near-significant main effect of pre-stress drug treatment was found for Arc-ir cell counts in the AI ($P = 0.055$), replicating the findings of the previous study and validating a relatively novel method for counting cells used in this study. Second, a trend toward significance was seen regarding main effect of pre-stress guanfacine for active CaMKIIα-ir cell counts in the AI ($P = 0.093$); this novel finding suggests that guanfacine may be lowering the activity of CaMKIIα-ir neurons in the AI. An understanding of the potential cell-type specific mechanisms by which guanfacine affects behavioral change in male mice is critical to understanding how guanfacine may be used to prevent relapse in human smokers.

Glossary

Below is a list of terminology and abbreviations used in this thesis, as well as their respective definitions. Terms are listed in the order of appearance in the thesis.

Guanfacine	An α_2 adrenergic receptor (α_2-AR) agonist
Nicotine CPP	Nicotine conditioned place preference; a preclinical model of drug-seeking behavior
Stress-induced reinstatement	A reinstatement of previously extinguished drug-seeking behavior after a stressor; a preclinical analog of stress-induced relapse
Arc	A protein marker of active cells
Immunohistochemistry	A technique used to label particular proteins in thin sections of tissue with fluorescent markers that can then be detected with fluorescent microscopy
Immunoreactive	Displaying a fluorescent signal for a particular protein
AI	Anterior insular cortex
Glutamatergic neurons	Neurons that release an excitatory neurotransmitter
GABAergic neurons	Neurons that release an inhibitory neurotransmitter
CaMKIIα	Calcium/calmodulin-dependent protein kinase IIα; a protein marker of glutamatergic neurons
PV	Parvalbumin; a protein marker of a subtype of GABAergic neurons
Z-stack	A stack of focal planes in the z-dimension that are a set distance apart (1 μm apart for this experiment)
ROI	Region of interest; for this experiment, the volume in the AI that was imaged, and within which cells were counted

1. Introduction

1.1 Background on smoking

Tobacco smoking constitutes a significant public health burden worldwide, accounting for more than 7 million deaths per year (World Health Organization, 2017). In the United States specifically, tobacco smoking is responsible for approximately 1 in 5 deaths annually, or approximately 1,300 deaths per day (U.S. Department of Health and Human Services, 2014). In the United States, tobacco smoking has constituted the leading cause of preventable disease and death for many years (Centers for Disease Control and Prevention, 2019).

It is important to note that for every person who dies because of smoking, at least 30 are currently living with a serious smoking-related illness. According to the 2014 U.S. Surgeon General's report, smoking has been known to lead to disease and disability in nearly every organ of the body, with new adverse health outcomes regularly being added to the list (U.S. Department of Health and Human Services, 2014). Despite increasing public awareness of these health risks, many adults—currently, approximately 14% in the United States—continue to smoke because addictions are defined, in part, by the inability of the user to successfully quit despite known adverse consequences (CDC, 2019).

Just considering tobacco smoking, however, ignores an important modern day issue. Looking at overall tobacco product use among adults, the usage jumps from 14% (for just tobacco smoking) to 20% (CDC, 2017). Much of the difference between these two values can be attributed to steadily increasing numbers of adults using e-cigarettes, which were introduced to the U.S. in the mid-2000s (Wang et al, 2018).

Shifting the focus away from adult tobacco users, the most concerning numbers for e-cigarette use come from young users. The most recent numbers show that in 2019, 10.5% of

middle school students and 27.5% of high school students report using an e-cigarette in the past 30 days; this is more than a threefold increase from 2018 (Cullen et al, 2019). Importantly, though some e-cigarettes are marketed as nicotine-free, 99% of all e-cigarettes do in fact contain nicotine, the same primary addictive ingredient found in traditional tobacco cigarettes and other tobacco products (CDC, 2020). While e-cigarette use may be a way to reduce harm in dependent adult smokers, uptake of nicotine use during adolescence can alter behavior, increase likelihood of later cannabis use, and increase frequency and amount of later cigarette smoking (Ksinan et al, 2020; National Academy of Medicine, 2018). Thus, the issue of nicotine addiction is far from being a problem of the past, and continues to plague our modern day society.

1.2 Nicotine addiction and stress-induced relapse

Nicotine is the primary addictive ingredient in tobacco products, and the tenacity and cyclicity of nicotine addiction among cigarette smokers has been well characterized. Beginning with an initial exposure to nicotine, drug use escalates from infrequent use to chronic use (Cleck & Blendy, 2008). When an individual is in a state of chronic drug use, periods of abstinence are accompanied by symptoms of withdrawal, which for nicotine include irritability, restlessness, and depression, among others (CDC, 1994). In a majority of cases, withdrawal is followed by a relapse back to drug use, constituting a vicious and tenacious cycle.

Although many adult cigarette smokers want to quit, they become trapped in this cycle, and very few are able to enter long-term abstinence successfully. Approximately 70% of adult cigarette smokers express a desire to quit smoking, and more than half of smokers make a quit attempt lasting more than one day, but only about 7.5% are successful in quitting (CDC, 2019). This highlights the need for a better understanding of relapse behavior, and its underlying mechanisms. Stress is one important and common mechanism that promotes relapse to

smoking—thus, stress-induced relapse to nicotine use (also known as stress-induced reinstatement, in the context of laboratory studies), and potential therapies to attenuate stress-induced relapse, have been the subject of much research in the field in recent years.

Stress can exert its influence through several neurotransmitter systems, including noradrenaline (Koob, 2008). Accordingly, both clinical and preclinical research have shown that noradrenergic agents can affect stress-induced reinstatement of drug seeking, including for nicotine. In particular, α_2-adrenergic receptor (α_2-AR) agonists have been shown to reduce stress-induced smoking in human smokers (McKee et al., 2015; Covey & Glassman, 1991), as well as reduce stress-induced reinstatement of nicotine self-administration in male rodents (Zislis et al., 2007).

While clinical studies have used both clonidine (Covey & Glassman, 1991) and guanfacine (McKee et al., 2015), both of which are α_2-AR agonists, preclinical studies have only used clonidine (Zislis et al., 2007; Yamada & Bruijnzeel, 2011). Guanfacine, however, is more specific for the α_{2A}-AR subtype and thus has decreased risk of adverse side effects such as sedation and postural hypotension seen with clonidine (Arnsten, Cai, and Goldman-Rakic, 1988; Cahill et al., 2013). Further, guanfacine has demonstrated safety and efficacy in human patients as an FDA-approved medication for attention deficit hyperactivity disorder (Arnsten, 2010).

As an aside, it is worth noting that while guanfacine hadn't been used in a preclinical study to investigate its effect on stress-induced reinstatement of nicotine seeking, it has been used in preclinical studies outside of this particular context. For example, guanfacine has been used in preclinical models to study antidepressant effects (Mineur et al, 2015) and stress-induced reinstatement of other drugs such as cocaine (Perez et al, 2020), but not nicotine specifically.

1.3 Previous study from our lab

Accordingly, previous work in our lab (the Picciotto Lab at the Yale School of Medicine) has used a mouse model to investigate whether guanfacine attenuates stress-induced relapse, or reinstatement, of nicotine conditioned place preference (CPP). Nicotine CPP is a preclinical model that involves quantifying drug seeking behavior by measuring the time a subject spends in a chamber in which they had received nicotine injections relative to a chamber in which they had received saline injections. After a period of abstinence and extinction, during which the preference for the nicotine chamber is extinguished, the mouse is given a stressor, in this case a forced swim, and the reinstated preference for the nicotine chamber (a stress-induced reinstatement effect) is measured. Giving a guanfacine injection, compared to saline as a control, prior to the stressor allows for investigation of whether guanfacine can decrease stress-induced reinstatement.

This study found that guanfacine attenuates stress-induced reinstatement of nicotine CPP in both male and female mice (Lee et al., 2019). In addition to these findings, this paper also probed the associated changes in brain activity that might be associated with these behavioral findings; using a mouse model is useful in this regard. To investigate the effect of guanfacine in the brain, this study used immunohistochemical staining of brain tissue samples for the Arc protein, which is a marker of neuronal activity (Lyford et al., 1995). Cells that are positive for Arc, as indicated by fluorescent signal following immunohistochemistry (i.e. Arc-immunoreactive cells), are thought to be recently active cells. Thus, this approach allowed for identification of brain regions in which guanfacine may play a role and alter neuronal activity.

Immunohistochemistry results indicated that in the anterior insular cortex (AI), guanfacine decreased the number of Arc-immunoreactive cells in male mice overall, as

determined from automated counting of cells in a 2D plane (Lee et al., 2019). The AI is a region of the brain has been shown to play an important role in addiction to cigarette smoking, and a theoretical framework proposes that the insula represents the interoceptive effects (that is, the feeling within the body) of drug taking (Brody et al, 2002; Naqvi, Rudrauf, Damasio, & Bechara, 2007; Naqvi and Bechara, 2010). However, because Arc is a measure of activity in any neuronal type, it is unknown from this study which specific cell types guanfacine may be acting on. An analogy of a metal detector could be useful here: this previous study from the lab told us where over a large area of the brain to look in particular (i.e. focus further investigation in the AI region), but it doesn't tell us what's "underneath" (i.e. what cell types are being acted upon). Gaining this level of mechanistic insight is the goal of the present study.

1.4 The Present Study

The present study builds upon the findings of the initial study from my lab (Lee et al., 2019), and aims to probe cell-type specific activity in order to provide greater mechanistic understanding of the finding that guanfacine decreased overall neuronal activity in the AI of male mice when administered before a swim stress. Gaining this level of mechanistic insight is critical for developing a novel therapeutic tool to aid in smoking cessation in humans.

Specifically, I will be looking at two particular populations of cell types: glutamatergic and GABAergic neurons, which release excitatory and inhibitory neurotransmitters, respectively. Just as in the previous experiment, immunohistochemistry is a useful tool to investigate the activity of these particular cell types. Calcium/calmodulin-dependent protein kinase IIα (CaMKIIα) is a protein present in glutamatergic cells (Jones, Hentley, & Benson, 1994). Parvalbumin (PV) is a protein present in a subtype of GABAergic cells (Xiangmin et al., 2009). Thus, by looking at the activity of CaMKIIα-immunoreactive cells (CaMKIIα-ir) and PV-ir cells

in the AI region of male mice, I hope to glean mechanistic insight into how guanfacine attenuates reinstatement of nicotine CPP in these male mice.

I chose to look at glutamatergic (i.e. CaMKIIα-ir) and GABAergic neurons as they are the two broad classes of neurons in the brain, and are a good starting point for investigations of cell-type specific activity. As mentioned before, there are distinct subpopulations of GABAergic neurons in the brain, of which one subtype is the PV-ir GABAergic neurons (Kubota, Hattori, & Yui, 1994). I chose specifically to investigate PV-ir neurons, as previous studies point to the stress response in the brain involving alterations in the activity of PV-ir GABAergic neurons, particularly in the medial prefrontal cortex (McKlveen et al, 2016). Since guanfacine specifically acts on the noradrenergic pathways on the brain, which is one of the neurotransmitter systems important in the brain's stress response, it is reasonable to hypothesize that in the AI, guanfacine may impact the activity of PV-ir neurons.

It is important to note that previous studies have also elucidated sex differences in the alterations of PV-ir neuron activity in the stress response, particularly in the prefrontal cortex and limbic regions (Shepard, Page, & Coutellier, 2016). In the realm of stress-induced reinstatement, previous findings from our lab have already elucidated an initial sex difference: guanfacine (which acts on the stress pathways in the brain) lowers activity of neurons in the AI of male mice, but not female mice (Lee et al., 2019). Thus, when investigating cell-type specific mechanisms by which guanfacine is acting, it becomes important to do so in a sex-specific manner. For the sake of feasibility, my study follows up only on male mice, but future experiments should involve female mice, to provide a comparison for investigation of sex differences.

Given the links made by previous studies between stress and alterations in PV-ir neuron activity, my hypothesis is that in male mice, guanfacine specifically increases the activity of PV-ir neurons in the AI, increasing their inhibitory activity such that they cause powerful inhibition of other excitatory (glutamatergic, or CaMKIIα-ir) neurons. Since PV neurons can inhibit glutamatergic neurons in a network effect, this could cause an overall decrease in neuronal activity in the AI, confirming previous findings (Lee et al., 2019). The next section (specifically, the second objective) will describe in more detail how the combination of immunohistochemistry and following analysis of co-localized cells will allow me to explore this hypothesis.

1.4.1 Objectives

This study had two objectives. The first was to replicate the finding that guanfacine reduces activity in the AI when administered in male mice before a stressor. However, while the previous study involved counting Arc-ir cells in the AI across a 2D plane in the brain tissue section, my study involved counting cells in the AI in a 3D region of defined volume.

The previous study looked at a 2D section of a tissue region, in which cells across the ~40 micrometer tissue section are collapsed into a 2D plane (Lee et al., 2019); however, this approach is disadvantageous specifically for co-localization, as two different cells that are located in the same location in the x-y plane but at different depths through the tissue section may appear to be the same cell, when viewed in a collapsed x-y plane. This is problematic for co-localization, as two different cells that are located at different depths, and expressing two different markers, may appear to be a single cell with a co-localized signal. Due to this disadvantage, I chose to collect a z-stack, capturing images at different focal planes (1 micrometer apart) throughout the depth of the tissue. This allows me to investigate co-localization in each separate plane, avoiding the aforementioned issue.

However, while for 2D regions there are established and well-validated tools for automated cell counting in ImageJ, an open-source image analysis software from the NIH, such methods are lacking for counting cells in 3D. Because manually counting cells across a 3D z-stack is time-consuming, and establishing standardized criteria and protocols for manual counting is labor-intensive, the standard in the field has been to count cells across a 2D region, as had been done in the previous study in my lab (Lee et al, 2019). To our knowledge, manual counting of cells across a z-stack is a method that has been used very rarely in the literature (see Ikeda et al, 2017 for one example), and so verification of this method by replication of previous findings from my lab was important. If this method is validated, the criteria used to delineate cells manually (e.g. average size, sphericity, etc.) can perhaps be applied to develop an accurate 3D automated counter, or possibly a deep learning tool in the future.

The second objective, as previously discussed, was to investigate how guanfacine alters the activity of CaMKIIα-ir and PV-ir neurons in the AI in male mice. As mentioned before, data from the previous study from my lab shows that in male mice, Arc-ir neurons are decreased in the guanfacine injection condition compared to the saline condition (i.e. significant main effect of pre-stress drug treatment), but this data doesn't say whether inhibitory or excitatory neuronal activity is decreased. I will examine CaMKIIα-ir and PV-ir neuron activity in male mice in this brain region to gain cell-type-specific mechanistic insight.

The primary method to investigate this objective is immunohistochemistry, which will allow me to classify cells as Arc-ir, CaMKIIα-ir, and PV-ir based on their fluorescent signals. In order to investigate the number of *active* CaMKIIα-ir and *active* PV-ir cells in the AI, I will rely on co-localization of signal following immunohistochemical experiments: co-localized Arc-ir

and CaMKIIα-ir cells indicate active CaMKIIα-ir cells, and co-localized Arc-ir and PV-ir cells indicate active PV-ir cells.

I predict that I will find the following in male mice who are given a guanfacine injection prior to a stressor: there will be an increase in the number of active PV-ir neurons (a subtype of GABAergic neurons; inhibitory), causing network inhibition and a decreased number of active CaMKIIα-ir neurons (glutamatergic; excitatory), resulting in an overall decrease in neuronal activity in the AI.

2. Methods

2.1 Animals

Male and female C3H/HeJ mice were obtained from The Jackson Laboratory (Bar Harbor, Maine) at 6-10 weeks of age, and tested at 10-12 weeks of age, following at least 1 week of acclimation. Mice were group-housed, maintained on a 12-hour light-dark cycle (lights on at 7:00 AM), and provided standard chow and water *ad libitum*. All procedures were approved by the Yale University Institutional Animal Care and Use Committee.

2.2 Design

This experiment consists of, in order: behavioral conditioning (nicotine CPP), tissue collection, immunohistochemical staining, microscopic imaging of fluorescent markers, counting of Arc-ir cells and co-localized cells, and data analysis (Figure 1). Nicotine CPP was conducted for male mice in a 2 (nicotine- vs. saline-conditioned) x 2 (guanfacine vs. saline treatment prior to stress) design. Following behavioral conditioning and tissue collection, the immunohistochemical staining, imaging, cell counting, and data analysis for the male mice were conducted in the same 2 x 2 design. Each of these steps will be explained in further detail below.

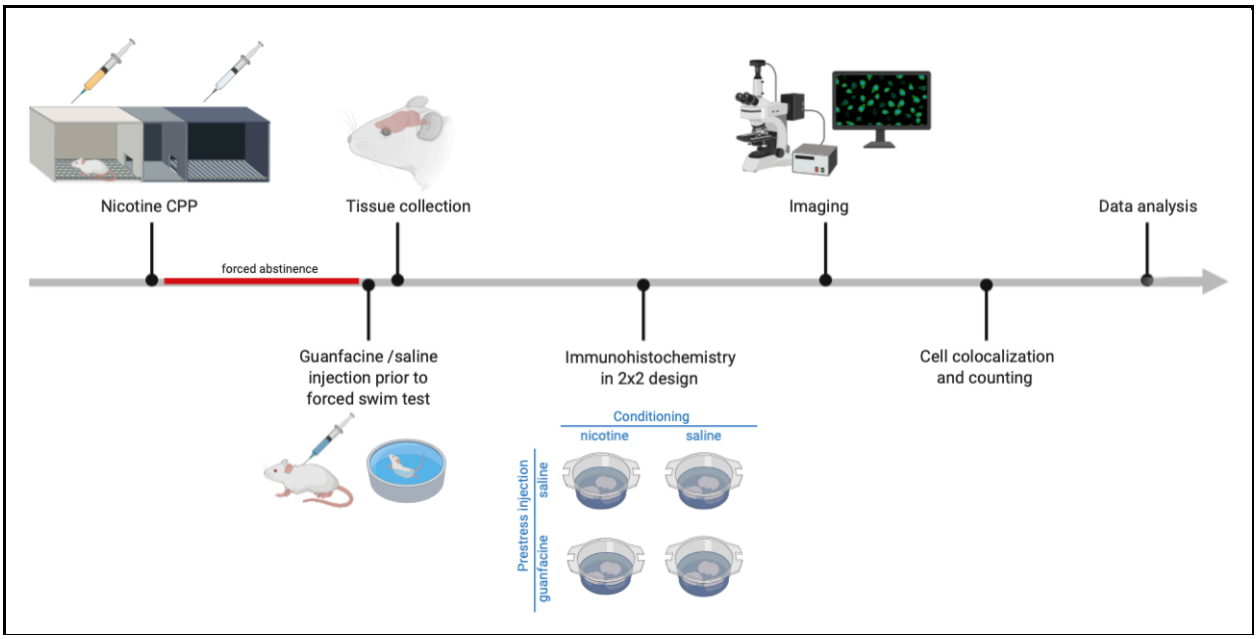

Figure 1: Schematic of experimental design, from nicotine CPP through data analysis.

2.3 Experimental procedure

2.3.1 Nicotine Conditioned Place Preference

All behavioral testing took place in an isolated room, with only the experimenter present. Each day, mice were transferred to the testing room and allowed 30 minutes of acclimation before handling or testing.

The first three days of the CPP procedure consisted of handling: mice were handled (as described in Grabus et al, 2006), and habituated to the syringe (without needle), which was applied to the back of the neck as if administering a subcutaneous injection. For the next six days, mice were conditioned in two distinct contexts with subcutaneous injections of nicotine or saline in alternating contexts for 30 min/day over 6 days. Control mice were conditioned with saline in both contexts. Based on the Lee et al (2019) study examining dose-response relationships for stress-induced reinstatement of nicotine CPP in male and female mice, nicotine CPP included administration of 0.5 mg/kg of nicotine to train male mice; saline was

administered in the same amount. The blood plasma concentration of nicotine after such an injection in mice is approximately equal to the average peak plasma levels of nicotine from a typical cigarette in humans (Lefever et al, 2017; Matta et al, 2006). Following this conditioning, mice were subjected to 2 weeks of forced abstinence, after which they were administered an injection of guanfacine (0.15 mg/kg) or saline followed 30 min later by a forced swim stress.

It is important to note that the same cohort of mice was used for the experiments in this paper and the immunohistochemistry experiments from the previously published paper from Lee et al. In this cohort, quantitative measurements of context preference were not taken as part of the behavioral CPP procedure, though the training procedure itself was identical to that used in an independent cohort of mice, from which behavioral measurements were taken during the CPP procedure.

2.3.2 Tissue Collection

Ninety minutes after the forced swim stressor, mice were transcardially perfused with ice-cold 1X PBS (intended to clear out blood so it is not fixed in blood vessels, which may interfere with imaging), then ice-cold 4% paraformaldehyde; then, brains were collected. Brain tissue was collected 90 minutes following the forced swim test to allow for peak Arc protein expression. In this experimental design, the Arc signal reflects how the brain is primed for drug-seeking by the forced swim stressor in the absence or presence of guanfacine. Following collection, brains were postfixed in 4% paraformaldehyde overnight, then transferred to 30% sucrose in 1X PBS. Brains were sectioned into 40 micrometer-thick coronal sections and stored at 4 °C in 1X PBS with 0.02% sodium azide.

2.3.3 Immunohistochemistry

The immunohistochemical staining protocol described here was developed over several weeks, optimizing for signal across the three fluorescing markers at 60x imaging. Sections containing the anatomical region of interest (the AI) were selected from every 6th section of the entire brain for stereological counting. Primary antibody incubation occurred overnight at 4 °C in 1:1000 guinea pig anti-Arc, 1:2000 rabbit anti-PV, and 1:1000 mouse anti-CaMKIIα. Secondary antibody incubation occurred for 2 hours at room temperature in 1:1000 donkey anti-guinea pig AlexaFluor647, 1:2000 donkey anti-rabbit AlexaFluor488, and 1:1000 donkey anti-mouse AlexaFluor546. Sections were mounted on SuperFrost Plus glass slides, and coverslips were applied using a Fluoromount-G mounting solution. Each of six immunohistochemistry runs included an animal from each experimental group for a total n = 6 per group (i.e. n = 24 total, across all four conditions).

2.3.4 Imaging

Immunohistochemically stained brain sections were imaged with an Olympus FluoView FV10i confocal microscope with a 60x objective. The AI region was imaged for both hemispheres from at least two sections, using a brain atlas to determine the appropriate area, as shown in Fig 2 (Paxinos & Franklin, 2004). A 3D ROI from the AI region was imaged: a square region was delineated in the x-y dimensions, and then a z-stack consisting of 6 focal planes within this square region was selected to give a 3D volume. Figure 3 shows one focal plane within the square region. The imaged section was 416 micrometers (in the x-direction) by 409 micrometers (in the y-direction) by 6 micrometers (in the z-direction), for a total imaged volume of 1.02×10^6 micrometers cubed.

The location of the 6-focal-plane stack in the overall ~40 micrometer tissue section was based on where CaMKIIα staining was optimized, since this primary antibody had the least consistent penetration of the tissue. The different fluorescent markers, as seen on the fluorescent microscope during imaging, are shown in Fig 3. Each fluorescent marker was excited at, and emitted, a different wavelength of light, allowing for independent imaging of each marker within the same tissue, as well as easy identification of different markers in the resulting image. PV-ir cells fluoresce green, CaMKIIα-ir cells fluoresce red, and Arc-ir cells fluoresce blue; see Fig 3.

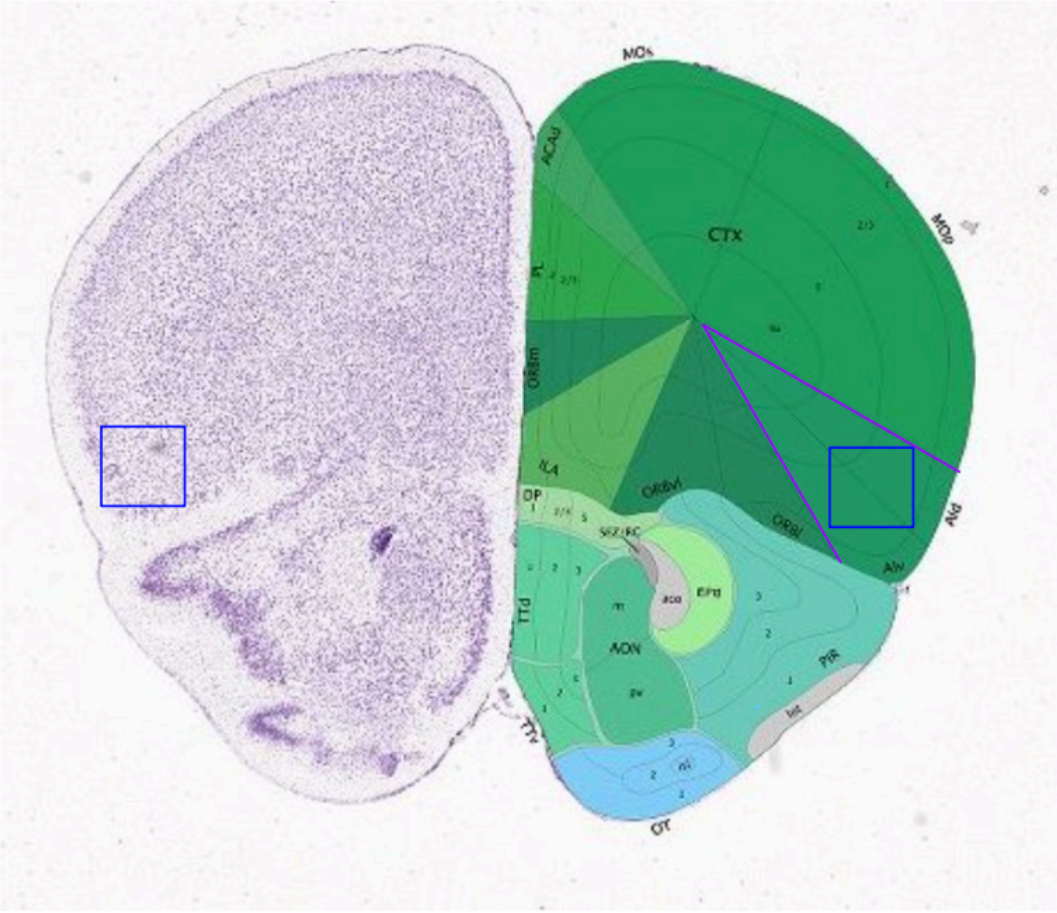

Figure 2: Location of the AI within a coronal section of the mouse brain. Wedge outlined in purple on the right side indicates the bounds of the AI region (identical bounds on left side). Boxes shown in blue on both the left and right sides indicate the square region that was imaged within the AI. Image adapted from The Allen Mouse Brain Atlas (2004). Bregma +2.045 mm.

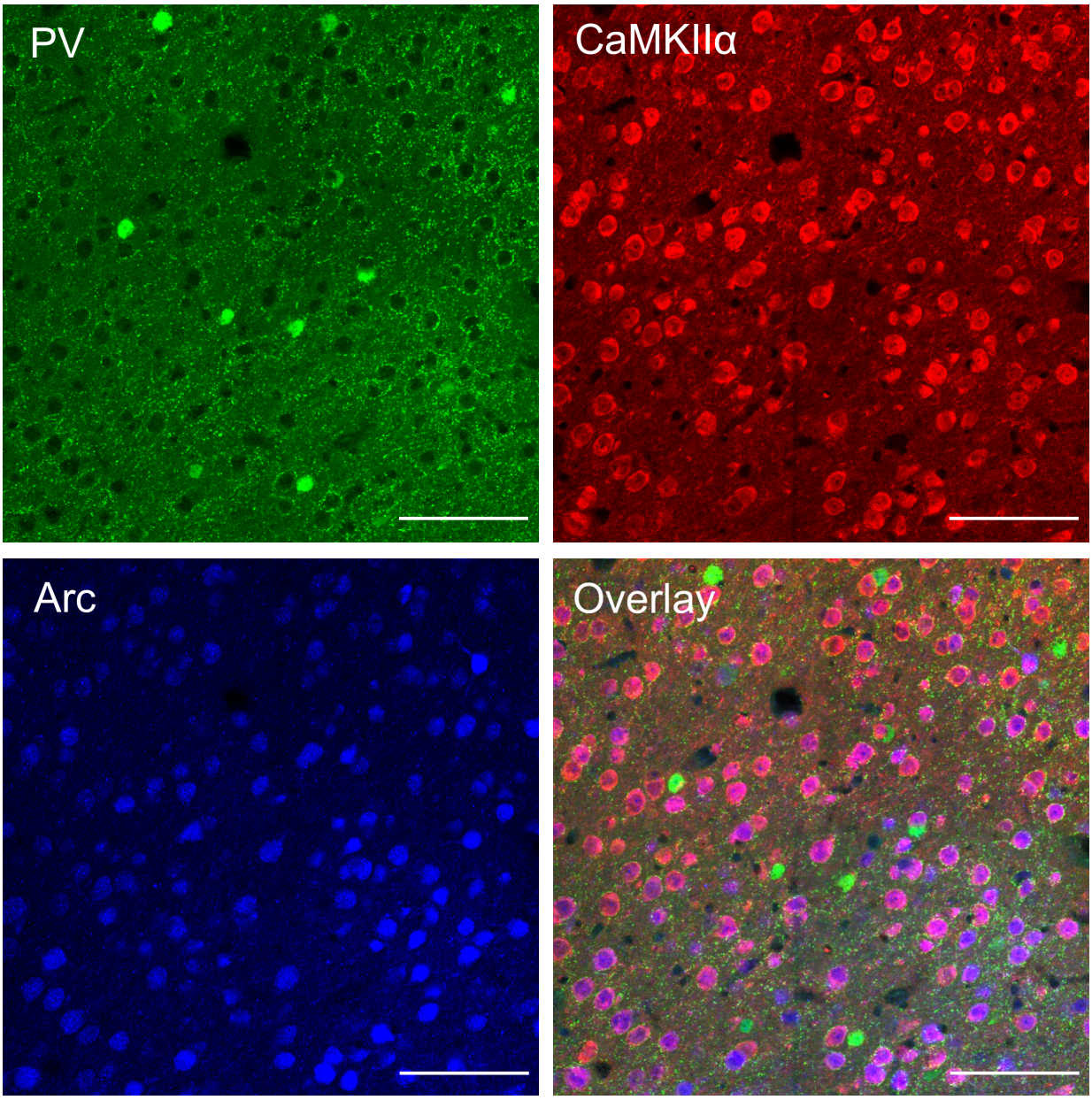

Figure 3: Individual fluorescent markers (PV, CaMKIIα, Arc) following immunohistochemistry on the fluorescent microscope, as well as the overlay of all three fluorescent markers. Scale bar 100 μm.

2.3.5 Cell co-localization and counting

Prior to generating co-localized cell files and initiating the counting protocol, all image files were blinded using a code generated in MATLAB.

For each imaged ROI, I constructed two new image files containing co-localized cells using ImageJ: (1) Arc-ir and CaMKIIα-ir co-localized cells, and (2) Arc-ir and PV-ir co-localized cells.

New image files containing co-localized cells were constructed as follows. First, a threshold was applied to each channel (corresponding to the individual fluorescent markers for which co-localization was being determined) of the ROI to create a binary image for each channel, using the MaxEntropy thresholding function within ImageJ. Cells expressing the fluorescent marker appeared white (binary intensity 1), with the background appearing black (binary intensity 0). To generate a co-localized image, the Image Calculator in ImageJ was used: the two individual channels were multiplied, such that the binary intensities were multiplied at each point in the image, in each focal plane. The result is that co-localized cells (with binary intensities of 1) in both channels would appear with a binary intensity of 1 in the newly constructed co-localized image. However, cells that only express one fluorescent marker should have binary intensities of 0 and 1 that multiply to 0, and thus would not appear in the co-localized image.

After generating these co-localized files for each ROI, three files were counted: (1) co-localized Arc-ir and CaMKIIα-ir cells, and (2) co-localized Arc-ir and PV-ir cells, and (3) Arc-ir cells. Prior to counting, the Arc-ir image files were converted to binary images to ensure consistency with the co-localized cell files.

The protocol for manual counting across the z-stack (6 focal planes) was established by taking into consideration average cell size and sphericity, as well as accounting for variability across different fluorescent markers. Two steps were implemented to verify accuracy and consistency of cell counts across images. First, I verified accuracy by comparing the manual

counts from one focal plane to those computed by an ImageJ automated calculator (no automatic tool accurately computed counts across focal planes, which as mentioned is one reason for the reliance on manual counts for counting across the z-stack); this verification was done for several sample image files, with <5% discrepancy between manual and automatic counts in each individual image. Second, to ensure consistency in my own cell-inclusion criteria across files, I created a standard document containing sample cells I had elected to include or exclude in my counting, based on the criteria elucidated before.

2.4 Dataset

The above co-localization and counting procedure was followed for the dataset obtained after exclusion of several ROI images due to two exclusion criteria; subsequent data analysis used the same dataset. First, image files were excluded if the CaMKIIα signal was poor, which was unfortunately the case for a small fraction of the files. Second, files were excluded if the 6-focal plane z-stack was located toward the end of the tissue section, as these files didn't have cells appearing evenly throughout the 6 focal planes. Since data analysis for the present study involved capturing absolute counts of cells, it was important to have files in which cells appeared evenly across all 6 focal planes, to ensure that the image files would most accurately represent the number of cells in the AI region within a standardized volume.

The resulting dataset includes n = 5 for the control+saline group, n = 3 for the control+guanfacine group, n = 3 for the nicotine+saline group, and n = 2 for the nicotine+guanfacine group, for a total of n = 13 subjects. Most animals had 1-2 imaged sections of the AI each, for a total of 21 images.

2.5 Data Analysis

For the first objective, looking at the number of Arc-ir cells in the AI across conditions, I conducted a 2-way ANOVA using conditioning group (nicotine vs. control) and drug administration pre-stress (guanfacine vs. saline) as between-subjects factors.

For the second objective, I looked at counts of co-localized Arc-ir+PV-ir cells and Arc-ir+CaMKIIα-ir cells across the groups using the same 2-way ANOVA analysis. To restate my hypothesis in terms of these co-localized counts, I predicted that guanfacine would increase the number of co-localized Arc-ir+PV-ir cells (i.e. increase the activity of PV-ir neurons), which would in turn result in a larger decrease in the number of Arc-ir+CaMKIIα-ir co-localized cells (i.e. the increasing activity of PV-ir neurons would result in a network inhibition of CaMKIIα-ir cells, decreasing their activity), such that the overall activity in the AI would decrease.

3. Results

3.1 Trends in overall activity

A 2-way ANOVA was conducted using conditioning group (nicotine vs. control) and pre-stress treatment (guanfacine vs. saline) as between-subjects factors in male mice. There was a near-significant main effect of pre-stress injection ($F_{(1,9)} = 4.86$, $P = 0.055$), but no significant main effect of conditioning group and no interaction effect (Fig 4A). This replicates the previously published data, which found a significant effect of pre-stress injection of guanfacine in male mice, but no significant main effect of conditioning group and no interaction effect (Fig 4B). The replication of previous findings validates the method of manual 3D counting of cells used for this study. Means and standard errors of the mean for the Arc counts across conditions are tabulated in Table 1.

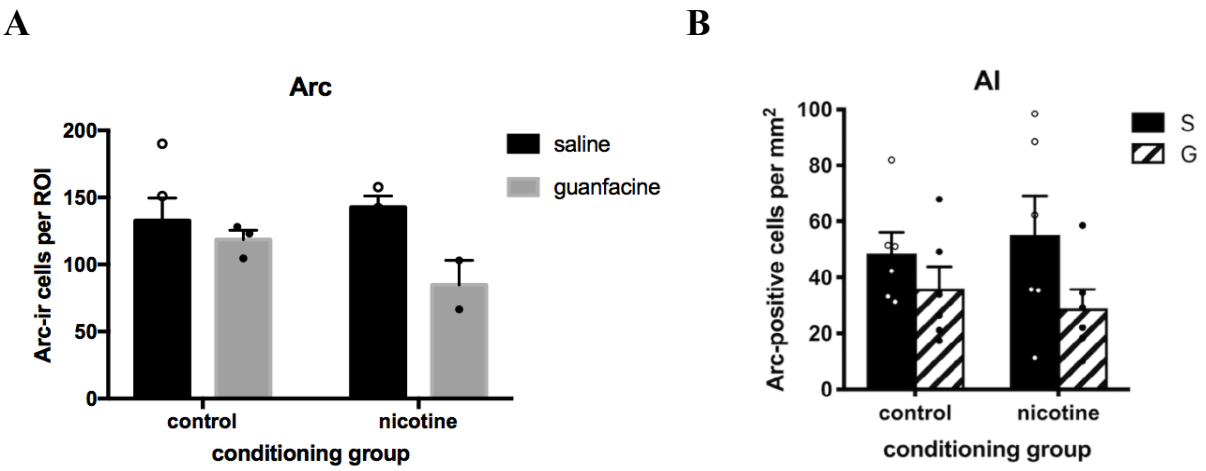

Figure 4: The finding that there is a near-significant effect of pre-stress administration of saline or guanfacine on Arc activity in the AI is replicated from previous published data. (**A)** Data from the present study obtained from manual counting of cells in a 3D ROI. (**B)** Previously published data (Lee et al., 2019), obtained from automated counting of a 2D section.

3.2 Trends in cell-type specific activity

Table 1 displays the means and standard errors of the mean for number of Arc-ir cells, number of co-localized Arc-ir+CaMKIIα-ir cells, and number of co-localized Arc-ir+PV-ir cells across the four conditions in the 2x2 design.

An important point to mention is that in my dataset, there were only three image files containing co-localized Arc-ir+PV-ir cells, and each of these captured <5 co-localized cells (Table 1), which limits the conclusions that can be drawn regarding the effect of guanfacine on the PV-ir cell activity. Another important note is that the sum of the active CaMKIIα-ir cells and active PV-ir cells does not add up to the total number of active cells in any of the four conditions listed in Table 1 because CaMKIIα-ir and PV-ir cells represent a large fraction, but not the totality, of neurons in the brain (Table 1).

Table 1: Counts of Arc-ir, colocalized Arc-ir+CamKIIα-ir, and colocalized Arc-ir+PV-ir cells

	Condition			
	control+saline	control+guanfacine	nicotine+saline	nicotine+guanfacine
Average Arc-ir cells (± SEM)	132.7 (± 16.8)	118.5 (± 7.1)	138.3 (±5.0)	84.8 (±18.3)
Average Arc-ir+CamKIIα-ir cells (± SEM)	95.4 (± 14.3)	79.8 (± 10.0)	87.4 (± 14.4)	48.5 (±28.5)
Average Arc-ir+PV-ir cells (± SEM)	0 (± 0)	0 (± 0)	0.83 (± 0.60)	0 (± 0)

To analyze the co-localized cell counts tabulated above, a 2-way ANOVA was conducted using conditioning group and pre-stress drug injection as between-subjects factors in male mice for the co-localized Arc-ir+CaMKIIα-ir cell counts and the same analysis was used for the co-localized Arc-ir+PV-ir cell counts. For the co-localized Arc-ir+CaMKIIα-ir cells counts, there was a trend toward a significant main effect of pre-stress injection ($F_{(1,9)} = 3.54$, $P = 0.093$), but no significant main effect of conditioning group and no interaction effect (Fig 5A). There were no significant main effects or interactions for the co-localized Arc-ir+PV-ir cell counts (Fig 5B).

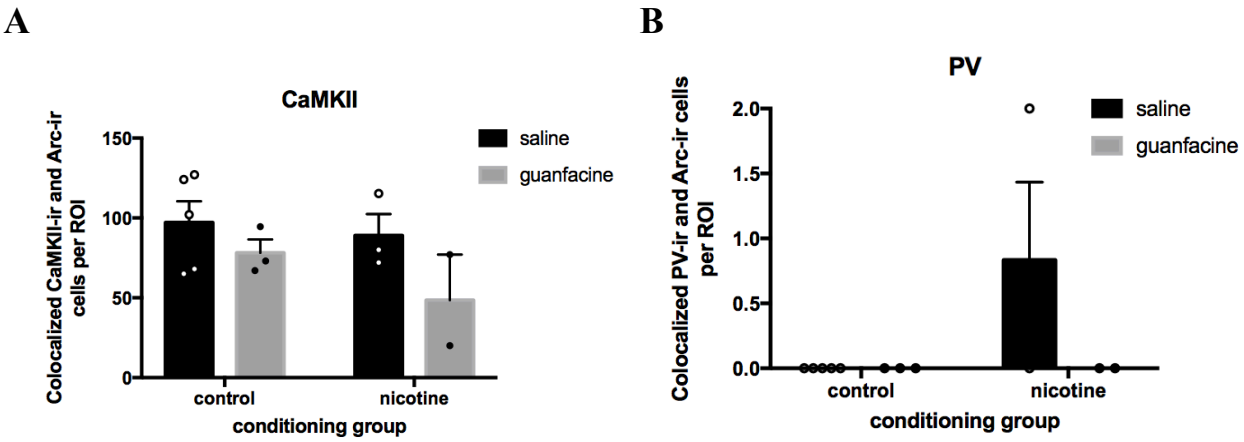

Figure 5: Counts of co-localized cells. (**A)** Counts of co-localized CaMKII-ir and Arc-ir cells. There was a trend toward a main effect of pre-stress drug injection ($P = 0.093$), but no significant main effect of conditioning group and no interaction effect. **(B) C**ounts of co-localized PV-ir and Arc-ir cells. There were no significant main effects of conditioning group or pre-stress treatment and no interaction effect.

4. Discussion

4.1 General discussion and future directions

This study revealed two important findings. First, there is a near-significant main effect of pre-stress injection of guanfacine on Arc activity in the AI of male mice. This replicates previously published data (Lee et al, 2019), and importantly, in doing so validates a novel 3D cell counting strategy. My method of manual counting of 3D images of the AI is different from the previous method of automated cell counting within a 2D image, which is much more commonly used in the literature. Importantly, counting in 3D images is advantageous in analyses involving co-localization. The validation of my manual 3D counting method could provide a basis for the development of an automated 3D counting method or deep learning method, which integrates the criteria used for manual 3D counting.

The second portion of this study, and the one that investigates a novel experimental question, focused on cell-type specific activity in the AI, in order to understand the mechanistic underpinnings of guanfacine's ability to lower overall activity in the AI of male mice. The hypothesis was that guanfacine would increase PV-ir neuron activity, observed as an increased number of co-localized Arc-ir+PV-ir cells, which would in turn result in a larger decrease in the number of Arc-ir+CaMKIIα-ir co-localized cells.

One important, unexpected finding from this portion of the study was the scarcity of Arc-ir+PV-ir co-localized cells within the imaged volumes of the AI; of the reduced dataset, only 3 files had any co-localized cells, all with very few cells. As might be expected, I found no main effect of pre-stress drug treatment or conditioning group and no interaction effect within the co-localized Arc-ir+PV-ir cells. Although this finding suggests that guanfacine does not affect the activity of PV-ir neurons, it is possible that the present study did not capture enough co-localized

Arc-ir+PV-ir cells to be able to make a meaningful comparison across conditions. Or, it is theoretically possible that guanfacine does in fact alter the activity of PV-ir cells (in line with our hypothesis), but that active PV cells are not sufficiently labeled with the Arc antibody. From the data I obtained, these possibilities cannot be disentangled, and this is an important limitation of our study (discussed further in section 4.2).

Despite the lack of observed effect of guanfacine on PV-ir cell activity, its effects can be more clearly seen on the activity of CaMKIIα-ir cells. Here, the present study found that in co-localized Arc-ir+CaMKIIα-ir cells, the main effect of pre-stress guanfacine injection approaches significance. This effect had been predicted in our hypothesis, though I had specifically predicted that it was the increased activity of PV-ir cells that would cause this effect. While this finding was not significant at $\alpha = 0.05$, it is notable that the trend appeared in such a small sample size, and thus a discussion of possible explanations for this trend is warranted.

Figure 6 below shows a schematic of four possible explanations I put forth to explain this observed trend. Importantly, each explanation converges on the same endpoint: that in male mice, the activity of CaMKIIα-ir cells within the AI is lowered by guanfacine treatment before stress. It is important to note that future experiments would be needed to support any one of these four explanations.

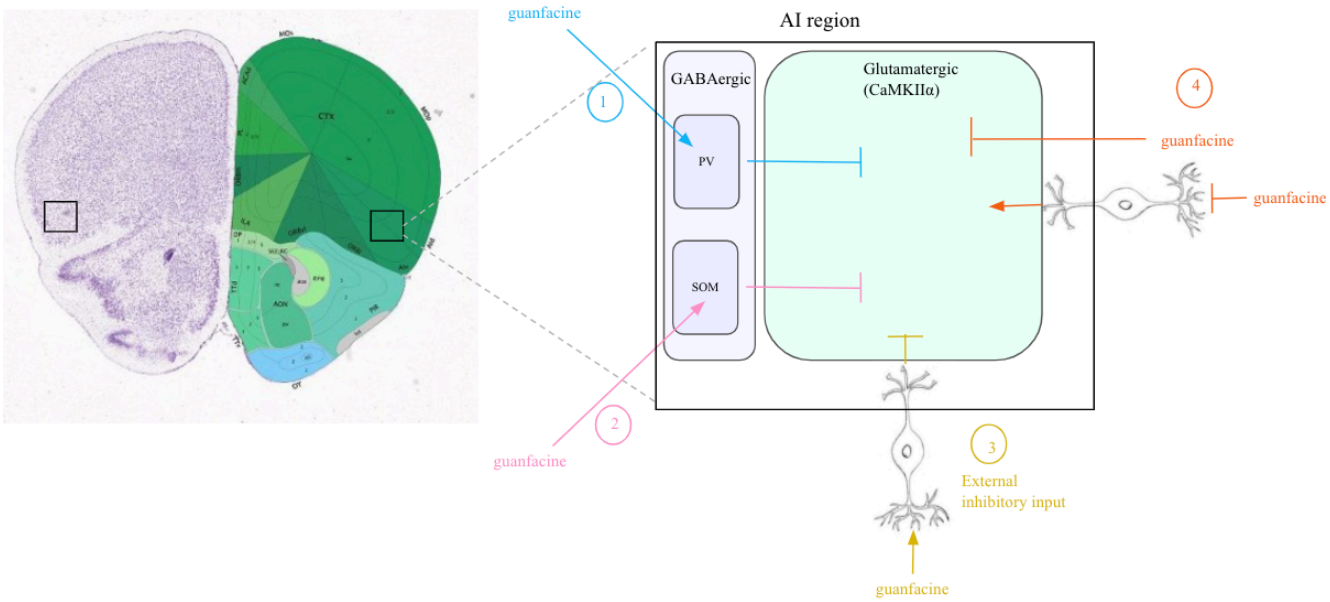

Figure 6: Potential explanations for the trend of lowered CaMKIIα activity in the AI region due to guanfacine treatment before stress. The AI region, as schematized by the black square, is enlarged (right). The two boxed regions inside indicate populations of GABAergic (purple) and glutamatergic (CaMKIIα-ir; green) neurons within the AI. GABAergic neurons are composed of subpopulations of cells (e.g. marked by the presence of PV, SOM, etc.) Numbers 1-4, also color-coded, indicate four potential explanations for the observed trend in our data. 1 (blue): guanfacine enhances the activity of PV-ir neurons in the AI region, which in turn inhibit the activity of CaMKIIα-ir neurons. 2 (pink): guanfacine enhances the activity of SOM-ir neurons in the AI region, which in turn inhibit the activity of CaMKIIα-ir neurons. 3 (yellow): guanfacine acts on inhibitory neurons outside the AI region to enhance their activity, which in turn project to CaMKIIα-ir neurons in the AI, inhibiting their activity. 4 (orange): guanfacine acts on excitatory rather than inhibitory neurons. Either guanfacine directly acts on CaMKIIα-ir neurons in the AI, lowering their activity, or guanfacine lowers the activity of CaMKIIα-ir neurons outside the AI which project to the CaMKIIα-ir neurons within the AI, having the net effect of lowering the activity of CaMKIIα-ir neurons in the AI.

The first possible explanation (Fig 6, blue) is that, in line with our hypothesis, guanfacine does in fact increase the activity of PV-ir neurons in the AI, and that this causes a decrease in the activity of CaMKIIα-ir cells in the AI. This hypothesis was based on literature demonstrating that guanfacine alleviates the effects of stress, and that a link has been drawn specifically between stress and alterations in PV-ir neuron activity (McKlveen et al, 2016). Given that this hypothesis is based on findings from previous literature, I maintain that it is a likely possibility. A follow-up study that captures more active PV-ir cells per group (i.e. by increasing sample size, by increasing imaged volume within the AI, or by using a different marker of neuronal activity) would be needed to support this possibility.

Another possibility (Fig 6, pink) considers other subtypes of GABAergic neurons in the brain. As mentioned before, PV-ir cells capture a subset of GABAergic cells, but not all. It is possible that guanfacine increases the activity of another subtype of GABAergic cells in the AI, such as the somatostatin-ir cells (SOM-ir), that were not captured in the data collected in this study. Then, the increased activity of SOM-ir cells could inhibit the activity of CaMKIIα-ir cells in the AI; this possibility is very similar to the original hypothesis, with the substitution of SOM-ir cells for PV-ir cells. This possibility could be tested in future experiments by repeating this experiment, and including immunohistochemical staining for other subpopulations of GABAergic cells.

A third possibility (Fig 6, yellow) considers the difference between intrinsic vs. extrinsic inhibition. The two possibilities considered so far postulate that guanfacine increases intrinsic inhibition within the AI—in other words, guanfacine increases the activity of inhibitory neurons within the AI. However, it is certainly possible that guanfacine enhances the activity of inhibitory cells outside the AI region (that wouldn't be captured in the imaged AI region); these cells could project to CaMKIIα-ir cells in the AI and decrease their activity, resulting in the observed trend. This would be a case of extrinsic inhibition of CaMKIIα-ir cells within the AI. Testing this possibility would likely rely on studies with different methods, perhaps involving tracing the projections from other neurons to the AI, or measuring circuit activity in real time.

Finally, while the above three hypotheses assume that guanfacine acts on inhibitory (GABAergic) cells, it is possible that guanfacine acts directly to inhibit excitatory cells. It may be paradoxical to conceptualize that guanfacine could increase the activity of inhibitory neurons or decrease the activity of excitatory neurons, but both are possibilities depending on what receptor subtypes and downstream signaling cascades are present in the cell. In the latter case,

option 4 (Fig 6, orange) shows that guanfacine may either directly lower the activity of CaMKIIα-ir cells in the AI, or lower the activity of CaMKIIα-ir cells that project to CaMKIIα-ir cells within the AI (thus functionally reducing the activity of CaMKIIα-ir cells in the AI).

To summarize, all four options mentioned above are consistent with the trend that was found in the present study. An important future direction would be to design experiments that would provide support for, or exclude, one of these four possibilities.

4.2 Limitations

There are a few limitations to note for this study. First and foremost, the study had a small sample size of n = 13 across all four conditions. In part, this small sample size resulted from the need to exclude a considerable fraction of ROIs due to poor CaMKIIα fluorescent signal. This issue could potentially be avoided in future by further optimizing the immunohistochemistry procedure for CaMKIIα signal, ensuring that fresh primary antibodies are used for each experiment (whereas usual lab procedure indicates that primary antibody can be reused several times), or using a different fluorescent marker for glutamatergic cells. Future experiments could thus aim for a full sample size of n=24, as the current study initially had prior to exclusion, which is consistent with previous studies in the literature and from our lab.

Second, this study limits its exploration to looking at the activity of CaMKIIα-ir and PV-ir cells for the sake of feasibility. However, this restriction excludes certain cell types from our analysis (e.g. SOM-ir GABAergic cells) that may be affected by guanfacine.

Finally, in the cohort of mice used for this study, quantitative measurements of context preference were not taken as part of the behavioral CPP procedure, though the training procedure itself was identical to that used in an independent cohort of mice, from which behavioral measurements were taken during the CPP procedure in the paper by Lee et al (2019). As a result,

while general comparisons can be made between the behavioral findings of the previous study and immunohistochemical findings of the current study, no direct correlations or connections can be drawn due to the different cohorts of mice used.

4.3 Concluding remarks

Overall, in suggesting that guanfacine lowers CaMKIIα-ir activity within the AI of male mice, this current study may fill in a piece of the puzzle of how guanfacine alters neuronal activity in the brains of male mice. Future research would be needed to evaluate female mice, as well as to unravel this mechanism more fully in both male and female mice. The goal of investigating the effect of guanfacine in the brains of both male and female mice is to understand how changes in brain activity mediated by guanfacine decreases stress-induced reinstatement in behavioral studies. A more detailed understanding of this mechanism, in addition to a more nuanced understanding of sex differences in terms of what is happening in the brain, will pave the way for the implementation of future large-scale clinical studies and ultimately will be helpful for the clinical implementation of guanfacine as a smoking-cessation medication.

Author Contributions

Ashna Aggarwal and Angela M. Lee (an MD/PhD graduate student in the lab) designed the current study, and developed the procedure for immunohistochemistry, imaging, and cell co-localization and counting. Angela Lee conducted the behavioral conditioning and tissue collection portion of the study, and Ashna Aggarwal completed all remaining steps of the study (immunohistochemistry, imaging, cell co-localization and counting, data analysis). Ashna Aggarwal wrote the manuscript for the current study, with helpful comments and suggestions provided by Angela Lee and Dr. Marina R. Picciotto. Angela Lee and Dr. Marina Picciotto provided advice on how to analyze and present the data.

Acknowledgments

I would like to express my gratitude to Angela Lee and Dr. Marina Picciotto for their invaluable help and guidance throughout the experimental process and writing stage. Their availability, patience, and encouragement over the last few years has been deeply appreciated. Angela Lee has been a dedicated mentor through the entire thesis process, and I am very grateful for her willingness to make time to help me with this project, even after she graduated from the lab this past year. Finally, I am grateful to the entire Cognitive Science Department, and especially Natalia Cordova-Sanchez, for facilitating the senior thesis process.

References

Allen Mouse Brain Atlas (2004). Retrieved from https://mouse.brain-map.org/static/atlas.

Arnsten AFT (2010). The use of α-2A adrenergic agonists for the treatment of attention-deficit/hyperactivity disorder. *Expert Rev Neurother* 10:1595–605.

Arnsten AFT, Cai JX & Goldman-Rakic PS (1988). The alpha-2 adrenergic agonist guanfacine improves memory in aged monkeys without sedative or hypotensive side effects: evidence for alpha-2 receptor subtypes. *J Neurosci* 8:4287–429 .

Bardo MT, Bevins RA (2000). Conditioned place preference: what does it add to our preclinical understanding of drug reward? *Psychopharmacology*, 153(1):31-43.

Brody AL, Mandelkern MA, London ED, Childress AR, Lee GS, Bota RG … Jarvik ME (2002). Brain metabolic changes during cigarette smoking. *Arch Gen Psychiatry*, 59(12):1162-1172.

Cahill K, Stevens S, Perera R & Lancaster T (2013) Pharmacological interventions for smoking cessation: an overview and network meta-analysis. *Cochrane Database Syst Rev*:1–50.

Center for Disease Control and Prevention (1994). Reasons for Tobacco Use and Symptoms of Nicotine Withdrawal Among Adolescent and Young Adult Tobacco Users — United States, 1993. Retrieved from https://www.cdc.gov/mmwr/PDF/wk/mm4341.pdf

Center for Disease Control and Prevention (2017). One in five US adults still using tobacco products in 2015. Retrieved from https://www.cdc.gov/media/releases/2017/p1109-tobacco-product-usage.html

Center for Disease Control and Prevention (2019). Smoking and Tobacco Use: Fast Facts. Retrieved from https://www.cdc.gov/tobacco/data_statistics/fact_sheets/fast_facts/index.htm.

Center for Disease Control and Prevention (2020). Quick facts on the risks of E-cigarettes for

kids, teens, and young adults. Retrieved from https://www.cdc.gov/tobacco/basic_information/e-cigarettes/Quick-Facts-on-the-Risks-of-E-cigarettes-for-Kids-Teens-and-Young-Adults.html#one

Cleck JN & Blendy JA (2008). Making a bad thing worse: adverse effects of stress on drug addiction. *J Clin Invest*, 118(2): 454-61.

Covey LS & Glassman AH (1991) A meta-analysis of double-blind placebo-controlled trials of clonidine for smoking cessation. *Br J Addict* 86:991–998.

Cullen KA, Gentzke AS, Sawdey MD, et al. e-Cigarette Use Among Youth in the United States, 2019. JAMA. Published online November 05, 2019. doi:10.1001/jama.2019.18387

Grabus SD, Martin BR, Brown SE, Damaj MI (2006). Nicotine place preference in the mouse: influences of prior handling, dose and strain and attenuation by nicotinic receptor antagonists. *Psychopharmacology*, 184(3–4):456-463.

Izeka MZ, Krentzel AA, Oliver TJ, Scarba GB, & Remage-Healey L (2017). Clustered organization and region-specific identities of estrogen-producing neurons in the forebrain of Zebra Finches (*Taeniopygia guttata*). *Journal of Comparative Neurology*, https://doi.org/10.1002/cne.24292

Jones EG, Huntley GW, Benson DL (1994) Alpha calcium/calmodulin-dependent protein kinase II selectively expressed in a subpopulation of excitatory neurons in monkey sensory-motor cortex: comparison with GAD-67 expression. *J Neurosci* 14:611-29

Ksinan AJ, Spindle TR, Thomas NS, Eisenberg T, & Dick DM (2020). E-cigarette use is prospectively associated with initiation of cannabis among college students. *Addictive Behaviors,* 106. https://doi.org/10.1016/j.addbeh.2020.106312

Koob GF (2008) A Role for brain stress systems in addiction. *Neuron* 59:11–34.

Kubota Y, Hattori R, Yui Y (1994). Three distinct subpopulations of GABAergic neurons in rat

frontal angular cortex. *Brain Research,* 649: 159-173.

Lee AM, Calarco CA, McKee SA, Mineur YS, & Picciotto MR (2019). Variability in nicotine conditioned place preference and stress-induced reinstatement in mice: Effect of sex, initial chamber preference, and guanfacine. *Genes, Brain, and Behavior*, https://doi: 10.1111/gbb.12601.

Lyford GL, Yamagata K, Kaufmann WE, et al. (1995) Arc, a growth factor and activity-regulated gene, encodes a novel cytoskeleton-associated protein that is enriched in neuronal dendrites. *Neuron* 14:433–445.

McKee SA, Potenza MN, Kober H, et al. (2015) A translational investigation targeting stress-reactivity and prefrontal cognitive control with guanfacine for smoking cessation. *J Psychopharmacol* 29:300–311.

McKlveen et al (2016). Chronic stress increases prefrontal inhibition: a mechanism for stress-induced prefrontal dysfunction. *Biol Psychiatry*, 80(10): 7544-764

National Academies of Sciences, Engineering, and Medicine (2018). *Public Health Consequences of E-Cigarettes*. Washington, DC: The National Academies Press. https://doi.org/10.17226/24952.

Naqvi NH, Rudrauf D, Damasio H, & Bechara A (2007). Damage to the insula disrupts addiction to cigarette smoking. *Science*, 315(5811):531-534.

Naqvi NH, Bechara A (2010) The insula and drug addiction: an interoceptive view of pleasure, urges, and decision-making. Brain Struct Funct 214:435–450.

Paxinos G and Franklin KBJ (2004) The Mouse Brain in Stereotaxic Coordinates, 2nd ed. Academic Press, NY

Shepard R, Page CE, Coutellier L (2016). Sensitivity of the prefrontal GABAergic system to chronic stress in male and female mice: relevance for sex differences in stress-related

disorders. *Neuroscience*, 332, 1-12

U.S. Department of Health and Human Services (2014). The health consequences of smoking—50 years of progress: A Report of the Surgeon General. Retrieved from https://www.ncbi.nlm.nih.gov/books/NBK179276/pdf/Bookshelf_NBK179276.pdf

Wang et al (2018). Tobacco product use among middle and high school students—United States, 2011-2017. *MMWR Morb Mortal Wkly Rep.* 67(22): 629-633.

World Health Organization (2017). WHO Report on the Global Tobacco Epidemic. Retrieved from https://www.who.int/tobacco/global_report/2017/en/.

Xiangmin X, Roby KD, & Callaway EM (2009) Immunochemical characterization of inhibitory mouse cortical neurons: Three chemically distinct classes of inhibitory cells. *J Comp Neurol* 518:389-404.

Yamada H & Bruijnzeel AW (2011) Stimulation of alpha-2 adrenergic receptors in the central nucleus of the amygdala attenuates stress-induced reinstatement of nicotine seeking in rates. *Neuropharmacology* 60:303-11.

Zislis G, Desai T V., Prado M, Shah HP & Bruijnzeel AW (2007) Effects of the CRF receptor antagonist d-Phe CRF(12-41) and the a2-adrenergic receptor agonist clonidine on stress-induced reinstatement of nicotine-seeking behavior in rats. *Neuropharmacology* 53:958–966.